

Direct observation of the femtosecond nonradiative dynamics of azulene in a molecular beam: The anomalous behavior in the isolated molecule

Eric W.-G. Diau, Steven De Feyter, and Ahmed H. Zewail

Citation: *J. Chem. Phys.* **110**, 9785 (1999); doi: 10.1063/1.478031

View online: <http://dx.doi.org/10.1063/1.478031>

View Table of Contents: <http://jcp.aip.org/resource/1/JCPSA6/v110/i20>

Published by the [American Institute of Physics](#).

Additional information on *J. Chem. Phys.*

Journal Homepage: <http://jcp.aip.org/>

Journal Information: http://jcp.aip.org/about/about_the_journal

Top downloads: http://jcp.aip.org/features/most_downloaded

Information for Authors: <http://jcp.aip.org/authors>

ADVERTISEMENT

Instruments for advanced science

Gas Analysis



- dynamic measurement of reaction gas streams
- catalysis and thermal analysis
- molecular beam studies
- dissolved species probes
- fermentation, environmental and ecological studies

Surface Science



- UHV TPD
- SIMS
- end point detection in ion beam etch
- elemental imaging - surface mapping

Plasma Diagnostics



- plasma source characterization
- etch and deposition process
- reaction kinetic studies
- analysis of neutral and radical species

Vacuum Analysis



- partial pressure measurement and control of process gases
- reactive sputter process control
- vacuum diagnostics
- vacuum coating process monitoring

contact Hiden Analytical for further details

HIDEN
ANALYTICAL

info@hideninc.com
www.HidenAnalytical.com

CLICK to view our product catalogue 

COMMUNICATIONS

Direct observation of the femtosecond nonradiative dynamics of azulene in a molecular beam: The anomalous behavior in the isolated moleculeEric W.-G. Diau, Steven De Feyter, and Ahmed H. Zewail^{a)}*Arthur Amos Noyes Laboratory of Chemical Physics, California Institute of Technology, Pasadena, California 91125*

(Received 27 January 1999; accepted 18 March 1999)

Using femtosecond-resolved mass spectrometry in a molecular beam, we report real-time observation of the nonradiative, anomalous dynamics of azulene. We studied both S_2 and S_1 state dynamics. The motion of the wave packet in S_1 involves two time scales, a dephasing time of less than 100 fs and a 900 ± 100 fs internal conversion. We discuss the dynamical picture in relation to the molecular structures and the conical intersection, and we compare with theory. © 1999 American Institute of Physics. [S0021-9606(99)02720-8]

I. INTRODUCTION

Almost 50 years ago, Beer and Longuet-Higgins¹ reported the anomalous fluorescence behavior of azulene, the deep blue hydrocarbon, in rigid and liquid media, and Viswanath and Kasha² confirmed its existence. Azulene emits much more strongly from the second excited singlet state (S_2) than from the first one (S_1); the quantum yield^{3,4} of S_2 is ~ 0.05 and S_1 is $\sim 10^{-6}$. This striking behavior is in violation of Kasha's rule, which would predict that emission of light for organic molecules in the condensed media will be from the lowest excited state of a given spin multiplicity. Since the 1950's, there have been numerous theoretical and experimental studies and the molecule has become central to the understanding of nonradiative decays in large molecules.

The energy gap between the ground state S_0 and S_1 is similar to that of S_1 and S_2 ($\sim 14\,000$ cm^{-1}). Accordingly, one expects the rate of nonradiative decay of $S_1 \rightarrow S_0$ and $S_2 \rightarrow S_1$ to be similar; $S_2 \rightarrow S_0$ rate is less than that of $S_2 \rightarrow S_1$ because of the energy gap. In the conventional statistical theory, the rate is given by Fermi's Golden rule (see Refs. 5 and 6 for reviews): $k_{nr} = (2\pi/\hbar)V^2F\rho$, where V is the coupling matrix element, F the Franck-Condon factor, and ρ the density of states. To account for the disparity of 4 orders of magnitude, different considerations of V , F , or ρ were invoked. However, it is difficult to quantify this large difference given the similarity of the vibronic structure and the energetics. In fact, in Longuet-Higgins' original paper, he suggested an "unconventional" mechanism, namely the intersection of the S_0 and S_1 potential energy surfaces.

The first time-resolved study of S_1 nonradiative decay came from the picosecond experiments of Rentzepis,⁷ who reported ~ 7 ps for azulene in liquids. With sub-picosecond time resolution, Ippen *et al.*⁸ reported 1.9 ± 0.1 ps. Many other, direct or indirect, studies were made and gave differ-

ent lifetimes. Even for experiments carried out at the same excitation wavelength and the same solvent, the rate was reported to be different. For example, Schwarzer *et al.*⁹ gave $\tau(S_1) = 1.0 \pm 0.1$ ps, while Ippen *et al.*⁸ gave $\tau = 1.9 \pm 0.2$ ps. Also, the effect of the medium is not fully understood, and in some cases give counterintuitive results.

In mixed crystals, careful measurements¹⁰ of the linewidth of the $S_1 \leftarrow S_0$ transition gave a corresponding mean lifetime of not less than 3.3 ps. Linewidth measurements in supersonic jets by three different groups estimated the lifetime, depending on the excess vibrational energy, to be 0.8–0.4 ps,¹¹ 1 ps,¹² and 1.1–0.3 ps,¹³ indicating that the decay slows down in the condensed phase. More recently, the dependence of the rates on excess energy was studied in solution with subpicosecond¹⁴ and femtosecond¹⁵ resolution. Despite the extensive literature over the past 30 years, there have not been direct measurements of the nonradiative dynamics of isolated azulene in a molecular beam. Such measurements are essential for any direct comparison with theoretical studies of the potential energy surfaces and of the dynamics.

In this communication, we report real-time observation of the femtosecond (fs) nonradiative dynamics of azulene in a molecular beam. Using fs-resolved mass spectrometry, we investigated the initial motion of the nuclear wave packet and the actual rate of nonradiative decay in the isolated molecule. Two excitation schemes to S_1 and S_2 were invoked, and we also studied the polarization behavior of the decay. Our results indicate that in isolated azulene, the time scale of the nonradiative decay cannot be picoseconds and is measured to be 900 ± 100 fs; see below. We discuss the dynamical picture in relation to molecular structures and the conical intersection (CI) of potential energy surfaces, originally proposed in 1955¹ and quantitatively computed in 1996.¹⁶ The study reported here offers the opportunity for elucidating the anomaly of the isolated molecule and the effect of the medium which is reflected in differences observed in the spectra

^{a)}Electronic mail: zewail@cco.caltech.edu

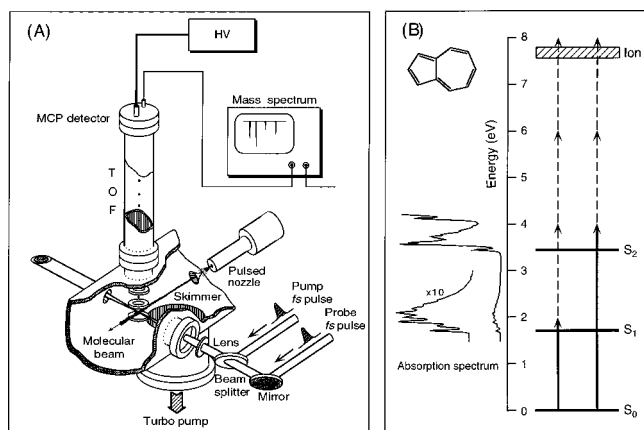


FIG. 1. (A) Femtosecond experimental arrangement with a pulsed molecular beam system combined with a time-of-flight mass spectrometer. (B) Absorption spectrum (left) and the femtosecond excitation scheme of azulene (right). The solid arrow represents the pump pulse and the dashed arrow the probe pulse. The absorption spectrum is that of a hexane solution. The gas-phase spectra are detailed in Refs. 12 and 17. Typical pulse width used was 60 fs and the energy was varied from 2 to 45 μJ . The red pulse was centered at 615 nm and the UV at 307 nm.

of gas phase,¹⁷ supersonic jets,^{11–13} mixed crystals,^{10,18–20} and liquids (for reviews, see Refs. 16 and 21, and 29–38).

II. RESULTS AND DISCUSSION

The fs laser and molecular beam apparatus have been described in detail elsewhere,²² and the arrangement is schematically shown in Fig. 1(A). The instrumental response function was determined by the *in situ* measuring of the multiphoton ionization of xenon, which allows the determination of time zero and the FWHM.^{22,23} With fs (615 nm) pulses, the mass spectrum of azulene is dominated by a single peak at 128 amu, the parent mass. The fragmentation is insignificant when compared with electron impact ionization (Fig. 2). From the absorption spectrum of azulene, shown in Fig. 1(B), it is clear that the S_1 dynamics can be interrogated by the 615 nm excitation. The multiphoton ionization (MPI) detection involves three probe-photons at 615 nm [Fig. 1(B)] for the one-color experiments, or two photons at 307 nm for the two-color experiments. The S_2 dynamics were investigated by excitation at 307 nm followed by the absorption of two probe-photons at 615 nm [Fig. 1(B)].

A. Probing the S_1 dynamics

Figure 2 (lower panel) shows the transients of azulene after excitation to S_1 with an excess vibrational energy of $\sim 2000\text{ cm}^{-1}$; both beams are polarized parallel to each other. The transient is characterized by a fs component (up to 300 fs) and a longer decay component ($\tau \sim 1\text{ ps}$), visually seen at both positive and negative delay times. The shape of the transient is symmetrical with respect to time zero. This is expected for the one-color experiments with the intensity of both beams nearly equal. Quantitative analysis of the transient was made by treating the decay as biexponential convoluted with the measured cross correlation (from the xenon ionization measurement it is $\sim 90\text{ fs}$). In so doing we obtained $\tau = 900 \pm 100\text{ fs}$ and a fast component with $\tau_f = 60\text{ fs}$;

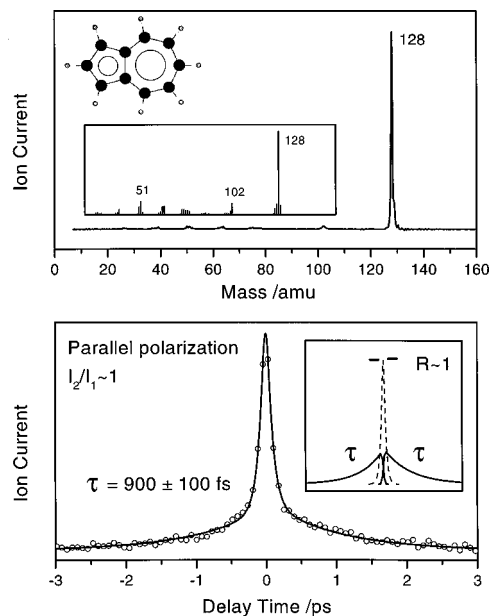


FIG. 2. (Top) Mass spectrum of azulene obtained with fs pulses. Only one distinct peak is shown at mass 128 amu. Inset shows the electron impact mass spectrum for comparison. (Bottom) Transient of one-color experiments (615 nm; parallel polarization) at similar probe and pump intensities ($I_2/I_1 = 21/19\ \mu\text{J}^{-1}$). The inset shows both fast (---) and slow decay (—) components obtained from the fitting procedure. The right and left bars represent the maximum signals deconvoluted at positive and negative delay times, respectively. The symmetry parameter R is nearly 1.

the cross correlation from the fit was very close to the measured one.²⁴ We define the ratio R as the amplitude of the τ -component at positive time to that at negative time. This ratio reflects the asymmetry and defines the magnitude of the signal on both sides of $t=0$.

The effects of power and polarization are illustrated in Fig. 3 (top). In contrast to the transient in the lower panel of Fig. 2 ($R \sim 1$) for equal powers, the long decay components at both sides of time zero in Fig. 3 do not appear as mirror images. Indeed, the amplitude of the long decay component at positive delay times is substantially larger than the one at negative delay times ($R \sim 1.7$). This increase parallels the increase of the ratio of I_2 to I_1 (~ 2), where I_1 (I_2) is defined as the intensity of the pump (probe) beam at positive delay times. Within the experimental uncertainties, the transients obtained for both the parallel and perpendicular polarizations and at the different intensities used give similar τ (Figs. 2 and 3).²⁵ As importantly, the shape indicates the correct scheme for pumping and probing S_1 and is in accord with the time ordering of the two pulses. The observed transients, therefore, provide the dynamics of S_1 with τ of 900 fs representing the average time for trajectory decay from S_1 to S_0 , as discussed below.

B. Probing the S_2 dynamics

The lower panel of Fig. 3 shows the transient obtained in the two-color experiments with a parallel polarization. The transient at positive and negative delay times reflects the dynamics of S_2 and S_1 , respectively. At positive delay times, molecules are excited to S_2 with a vibrational excess energy of $\sim 3800\text{ cm}^{-1}$ (307 nm). At negative delay times, mol-

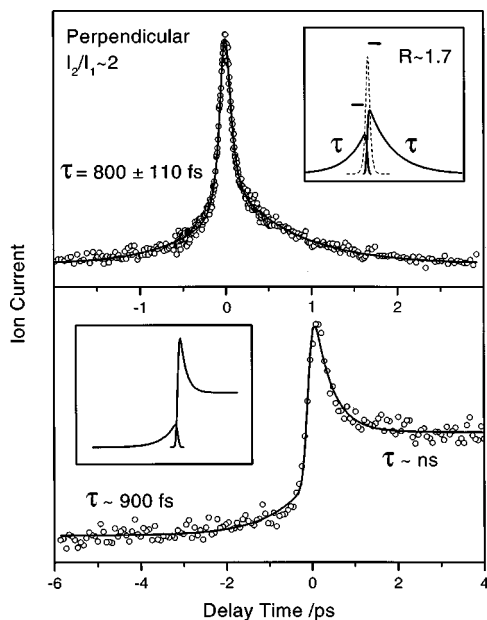


FIG. 3. (Top) Transient of one-color experiment with perpendicular polarization ($I_2/I_1=21/10 \mu\text{J}\sim 2$). The inset shows the fast- and slow-decay components on both sides of $t=0$ as defined in Fig. 2. (Bottom) Transient of two-color experiments with parallel polarization (pump at 307 nm/probe at 615 nm) and with different intensities ($2 \mu\text{J}/45 \mu\text{J}$); see the text for details. The right and left bars represent the maximum signals, as done in Fig. 2.

ecules are excited to S_1 (615 nm). Based on the results of Sec. II A, the decay at negative times for the two-color experiments should be 900 fs. Indeed, the fit in Fig. 3 (bottom) was fixed to 900 fs. The transient at positive delay times is entirely different, as it reflects the dynamics in the S_2 state: the transient is characterized by a fast (350 fs) and a very slow decay component, which does not show any significant decrease up to a delay of 60 ps. This >60 ps decay is consistent with previous work.²⁶ However, the appearance of the 350 fs decay is a direct manifestation of the nonradiative process, even in S_2 .

With an excess vibrational energy of 3800 cm^{-1} , we observed the nondecaying population up to a delay time of 60 ps; this represents the S_2 lifetime (~ 2 ns), as reported by Wallace²⁶ at an excess energy of 1950 cm^{-1} . The authors also found a fast decay component (<30 ps) at this high excess energy, which is the dephasing of the large number of levels excited at $t=0$ in what is known as dissipative intramolecular vibrational-energy redistribution (IVR).²⁷ Our results are entirely consistent with this general behavior.

C. Nonradiative dynamics and conical intersections

Since the first report on the anomalous fluorescence of azulene, most of the experimental results have been obtained in the condensed phase. The relaxation dynamics may involve solvent-induced vibrational relaxation, intramolecular vibrational-energy redistribution (IVR), and internal conversion (IC). However, in solution it is impossible to separate interstate electronic relaxation and medium-induced vibrational relaxation. In the gas phase, using molecular beam

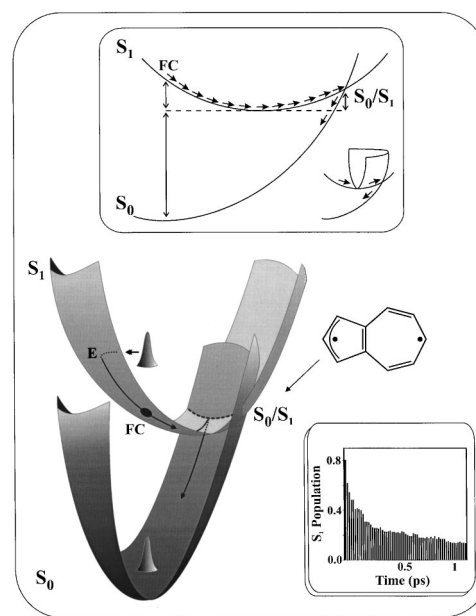


FIG. 4. F_s wave packet snapshots on the intersected potential energy surfaces. Shown are the molecular structures at the conical intersection and the calculated potential energy surfaces (Ref. 16); the bottom inset gives the results of the nonadiabatic dynamics simulation by Klein *et al.* (Ref. 28); see the text for discussion. FC is the Franck–Condon region reached by ground-state wave packet and E is the excess energy above this region.

techniques under collision-free conditions, the effect of IVR and IC, which are the cornerstones of the intramolecular dynamics, can be elucidated.

Originally, it was suggested¹ that the potential energy surfaces of S_0 and S_1 may intersect. In such a strong coupling limit, the standard theory (weak coupling limit) of nonradiative decay becomes not valid. Theoretical calculations¹⁶ have found a CI and a relaxation coordinate (RC) which connects the S_1 Franck–Condon geometry to the S_0 geometry at CI. This RC involves compression of the transannular bond together with expansion of the adjacent C–C bonds within the ring. Along this RC, the energy gap between S_0 and S_1 continues to shrink and ultimately leads to the S_0/S_1 CI (Fig. 4). The CI energy is calculated to be lower than that of the S_1 Franck–Condon geometry by a few kcal/mol¹⁶ (Fig. 4). Along the RC, the time required for the wave packet to move to the CI region is on the order of 10 fs and is independent of excess vibrational energy.¹⁶ According to this picture, all observed transitions, including the so-called origin, will undergo ultrafast IC; note that the true S_1 origin (Fig. 4) is far from the Franck–Condon vertical transition.

Following the fs preparation of the wave packet to the Franck–Condon region, the IC will be controlled only by the multiple crossings to S_0 , calculated by molecular dynamics and shown in Fig. 4; the results were obtained from nonadiabatic dynamics simulations based upon the mixed-state approach.²⁸ Funneling from S_1 into S_0 takes 900 fs and this CI picture is reminiscent of recent studies of another aromatic, pyridine.²³ At higher energies, the dephasing projects population on the RC, and this population passes through the CI by multiple crossings to the ground state. The entire dephasing process cannot exceed the observed 100 fs and represents the spread of the packet formed from all modes

excited. It is remarkable that the observed decay of 900 fs in the isolated azulene is in very good agreement with the trajectory calculations through the conical intersection and which reflect the steps involved in the multiple crossings to S_0 .

The S_1 lifetime inferred from linewidth measurements in supersonic jets varies from 0.3 ps to a few ps depending on the measurement and the wavelength of excitation. However, when considering the inhomogeneous contribution due to rotational congestion, the lifetime obtained from the studies of the groups of Amirav and Jortner,¹¹ Ito,¹² and Kenny¹³ is ~ 1 ps for the Franck–Condon origin excitation. Following the physical picture given in Fig. 4, the S_1 lifetime deduced from linewidth measurements represents an integration over time of IVR, the search for CI, and the crossings to S_0 . At higher excess energies, IVR may dominate the linewidth, especially if the Franck–Condon region is much different from the RC. Only at zero-excess energy can we relate the experimental slow-decay time to the *homogeneous* width; it is interesting to note that the MPI spectrum¹² clearly shows both sharp and broad background spectral regions.

Our value for the slow-decay component is a factor of 2 different from that of the solution phase,⁸ but similar to those reported in Refs. 9, 14, and 15 at the same wavelength and also in solution. The agreement indicates the ineffectiveness of the medium on the ultrafast crossings to the ground state, a feature which is understood given the strong coupling and the time scale of every crossing relative to the time for the solvent motion. Similarly, we can understand the lack of major changes for the rates upon deuteration, because of the unchanged S_0/S_1 coupling, and the decrease of rates in crystals because of the avoided crossing along RC.

The existence of the conical intersection and its dynamics can be rationalized by considering changes of molecular structures along the RC. Stretching the azulene in the ground state along the RC (Fig. 4) leads to a significant increase in energy as this motion destabilizes the structure due to the loss of resonance energy. Upon shortening of the transannular bond and lengthening of the adjacent C–C bonds, which leads to π -bond breakage and electronic resonance rearrangement, the structure becomes diradicaloid in nature. Because the $S_0 \rightarrow S_1$ is a $\pi-\pi^*$ transition, the energy of the antibonding orbital decreases while the bonding one increases along the RC until the S_1 minimum is reached, forming a diradicaloid structure. Further motion along the RC slightly increases the energy of S_1 which finally crosses to S_0 at the CI (Fig. 4). The similarity of the structures of S_1 and S_0 is critical for the effective coupling.

ACKNOWLEDGMENTS

This work was supported by the National Science Foundation and Office of Naval Research. S.D.F., a postdoctoral fellow of the Fund for Scientific Research–Flanders, acknowledges a Fulbright scholarship and financial support by the Katholieke Universiteit Leuven and by Caltech.

¹M. Beer and H. C. Longuet-Higgins, *J. Chem. Phys.* **23**, 1390 (1955).

²G. Viswanath and M. Kasha, *J. Chem. Phys.* **24**, 574 (1956).

³B. D. Wagner, D. Tittelbach-Helmrich, and R. P. Steer, *J. Phys. Chem.* **96**, 7904 (1992), and references therein.

⁴D. Huppert, J. Jortner, and P. M. Rentzepis, *J. Chem. Phys.* **56**, 4826 (1972).

⁵J. Jortner and S. Mukamel, in *The World of Quantum Chemistry: Proceedings of the First International Congress of Quantum Chemistry*, edited by R. Daudel and B. Pullman (Reidel, Dordrecht, 1974), p. 145.

⁶E. C. Lim, *Adv. Photochem.* **23**, 165 (1997).

⁷P. M. Rentzepis, *Chem. Phys. Lett.* **2**, 117 (1968).

⁸E. P. Ippen, C. V. Shank, and R. L. Woerner, *Chem. Phys. Lett.* **46**, 20 (1977).

⁹D. Schwarzer, J. Troe, and J. Schroeder, *Ber. Bunsenges. Phys. Chem.* **95**, 933 (1991).

¹⁰R. M. Hochstrasser and T.-Y. Li, *J. Mol. Spectrosc.* **41**, 297 (1972).

¹¹A. Amirav and J. Jortner, *J. Chem. Phys.* **81**, 4200 (1984).

¹²T. Suzuki and M. Ito, *J. Phys. Chem.* **91**, 3537 (1987).

¹³S. K. Kulkarni and J. E. Kenny, *J. Chem. Phys.* **89**, 4441 (1988).

¹⁴D. Tittelbach-Helmrich, B. D. Wagner, and R. P. Steer, *Can. J. Chem.* **73**, 303 (1995).

¹⁵A. J. Wurzer, T. Wilhelm, J. Piel, and E. Riedle, *Chem. Phys. Lett.* **299**, 296 (1999).

¹⁶M. J. Bearpark, F. Bernardi, S. Clifford, M. Olivucci, M. A. Robb, B. R. Smith, and T. Vreven, *J. Am. Chem. Soc.* **118**, 169 (1996).

¹⁷G. R. Hunt and I. G. Ross, *J. Mol. Spectrosc.* **9**, 50 (1962).

¹⁸J. M. Friedman and R. M. Hochstrasser, *Chem. Phys.* **6**, 145 (1974).

¹⁹G. J. Small and S. Kusserow, *J. Chem. Phys.* **60**, 1558 (1974).

²⁰R. M. Hochstrasser and C. A. Nyi, *J. Chem. Phys.* **70**, 1112 (1979).

²¹B. D. Wagner, M. Szymanski, and R. P. Steer, *J. Chem. Phys.* **98**, 301 (1993); see also Refs. 29–38.

²²A. H. Zewail, *Femtochemistry: Ultrafast Dynamics of the Chemical Bond* (World Scientific, Singapore, 1994), and references therein.

²³D. Zhong, E. W.-G. Diao, T. M. Bernhardt, S. De Feyter, J. D. Roberts, and A. H. Zewail, *Chem. Phys. Lett.* **298**, 129 (1998).

²⁴We also considered the fast component as a coherent spike due to the interference of the two pulses at $t=0$, and this gives $\tau=725$ fs. However, two observations support the biexponential analysis. First, the fitting for a coherent spike gives a deviation from the measured cross correlation at least by a factor of 2. Second, by changing the power we observed no major change in the ratio of the two components; for the parallel or perpendicular polarization this change is at most 20%. As expected, the fast-to-slow decay amplitude decreases as the polarization changes from parallel (4.6) to perpendicular (3). The appearance of the two components, fast and slow, is consistent with ionization of the initial wave packet on S_1 and at the crossing S_0/S_1 , reflecting the change in the cross section for ionization from pure S_1 to mixed S_0/S_1 state.

²⁵Note that for perpendicular polarization, τ is somewhat shorter (Fig. 3). However, within the uncertainties reported, the difference is not significant. We shall use the parallel values as the transients (Fig. 2) are clearly symmetric.

²⁶D. R. Demmer, J. W. Hager, G. W. Leach, and S. C. Wallace, *Chem. Phys. Lett.* **136**, 329 (1987).

²⁷P. M. Felker and A. H. Zewail, *Chem. Phys. Lett.* **108**, 303 (1984).

²⁸S. Klein, M. J. Bearpark, B. R. Smith, M. A. Robb, M. Olivucci, and F. Bernardi, *Chem. Phys. Lett.* **292**, 259 (1998).

²⁹E. Drent, G. Makkes van der Deijl, and P. J. Zandstra, *Chem. Phys. Lett.* **2**, 526 (1968).

³⁰P. M. Rentzepis, *Chem. Phys. Lett.* **3**, 717 (1969).

³¹J. P. Heritage and A. Penzkofer, *Chem. Phys. Lett.* **44**, 76 (1976).

³²P. Wirth, S. Schneider, and F. Dörr, *Chem. Phys. Lett.* **42**, 482 (1976).

³³D. Huppert and P. M. Rentzepis, in *Molecular Energy Transfer*, edited by R. D. Levine and J. Jortner (Wiley, New York, 1976), p. 270.

³⁴D. Huppert, J. Jortner, and P. M. Rentzepis, *Isr. J. Chem.* **16**, 277 (1977).

³⁵C. V. Shank, E. P. Ippen, O. Teschke, and R. L. Fork, *Chem. Phys. Lett.* **57**, 433 (1978).

³⁶E. T. J. Nibbering, K. Duppen, and D. A. Wiersma, in *Springer Series Chemical Physics, Vol. 53, Ultrafast Phenomena VII*, edited by C. B. Harris, E. P. Ippen, G. A. Mourou, and A. H. Zewail (Springer, Berlin/Heidelberg, 1990), p. 471.

³⁷T. Matsumoto, K. Ueda, and M. Tomita, *Chem. Phys. Lett.* **191**, 627 (1992).

³⁸D. Tittelbach-Helmrich, B. D. Wagner, and R. P. Steer, *Chem. Phys. Lett.* **209**, 464 (1993).